# Theoretical Study on the Mechanism of Ester Hydrolysis in Micellar Catalysis Using Model Systems

**Kenzi Hori,*[a] Akio Kamimura,[a] Junko Kimoto,[b] Sachiko Gotoh[b] and Yasuji Ihara[b]**
[a] *Department of Chemistry, Faculty of Liberal Arts, Yamaguchi University, Yamaguchi 753, Japan*
[b] *Yamaguchi Women's University, Sakurabatake, Yamaguchi 753, Japan*

A study has been made on the mechanism of ester hydrolysis in micellar catalysis, using model systems with *ab initio* MO calculations. The study ascertained that neutral imidazole cannot form a tetrahedral (TD) intermediate with esters since its basicity is very weak; the present MO calculations indicate that, immediately after its formation, the TD intermediate from *p*-nitrophenyl acetate and the imidazolyl anion decompose into *p*-nitrophenol and *N*-acetylimidazole. This accords with the experimental finding that *p*-nitrophenol is released quickly so that measuring the UV spectra of *p*-nitrophenol enables the reaction to be monitored. The TD intermediate formation step governs the enantioselectivity of micellar catalysis. *N*-Acetylimidazole reacts with the OH anion taken in from the liquid phase. We examined two paths for the decomposition: one similar to that of ester hydrolysis and the other the direct product formation of the acetate anion and imidazole. MP2/6-31+G//RHF/6-31G level calculations show that, in the activation energy, the latter mechanism is lower than the former by 7.5 kcal mol$^{-1}$.†

There are hydrophobic fields in the type of micelle which is constructed with surfactants. It is possible to make a system by adding peptides having a histidine residue to the field of micelles where the cosurfactants of the optically active peptide derivatives and cationic surfactants act as an enantioselective catalyst for ester hydrolysis.[1] The catalyst with an L-histidine residue, for example, enhanced the hydrolysis rate of *N*-benzyloxycarbonyl-L-amino acid *p*-nitrophenyl esters. The dipeptide catalyst, when modified, prompts hydration and stereorecognition for substrates to rise briskly.[2-4] We,[2] and other groups,[3,4] have been investigating the catalytic process in the cosurfactants, in which the hydrolysis, itself consisting of two processes, is expressed as follows:

$$C_{IM} + AcONp \xrightarrow{k_a} Ac\text{–}C_{IM} + p\text{-nitrophenol} \xrightarrow{k_m} C_{IM} + AcOH$$

where AcONp and $C_{IM}$ represent *p*-nitrophenyl ester and the imidazole catalyst, respectively, and Ac–$C_{IM}$ the acylated intermediate.

The first process consists of two steps. The initial step takes place in which the tetrahedral (TD) intermediate forms through the reaction of the AcONp and an imidazole fragment of the $C_{IM}$ histidine residue. The subsequent step includes the decomposition of the intermediate, forming *N*-acylimidazole and *p*-nitrophenol. Measuring the UV spectra of *p*-nitrophenol enables the reaction to be monitored, where we observed the pH dependence of the process:[5] in the pH region > 8 the decomposition rate of AcONp was accelerated strongly, for which the highly reactive imidazolyl anion was responsible. However, the reaction rate also increases at pH lower than 7. The carboxylate ion fragment in the peptide helps to increase the basicity of the imidazole moiety.

Models of an appropriate size need to be constructed for the study of hydrolysis in micelles, because real life experimental systems are too large to perform the *ab initio* molecular orbital (MO) calculations. *p*-Nitrophenyl acetate **1b** was, accordingly, adopted for the model of *p*-nitrophenyl esters. The experiments we performed suggest that imidazole and imidazolyl anion should be adopted for the model of $C_{IM}$ to make the calculations less cumbersome. The reactions of the first process are modelled as follows:

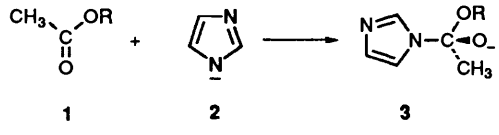

**1** **2** **3**

**a** R = $CH_3$ **b** R = $C_6H_4NO_2$ (1)

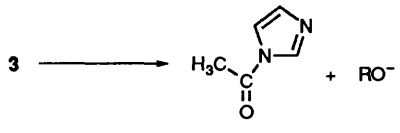

**4** (2)

Eqns. (1) and (2) show, respectively, the steps in which the TD intermediate **3** forms and decomposes.

In the second process Ac–$C_{IM}$ decomposes, as observed spectrophotometrically at 245 nm.[6,7] This second reaction corresponds to a hydroxy-mediated deacylation, though it is less stereoselective than the decomposition of AcONp.[6b] The model thus provides reactions for the process under consideration which are represented by eqns. (3) and (4).

There are two paths by which the decomposition of TD intermediate **5** takes place. One mechanism (4-1), resembling ester hydrolysis described in many textbooks, produces acetic acid and imidazolyl anions. The other (4-2) forms directly the acetate ion and imidazole by causing the imidazolyl fragment to extract a proton from the OH group in **5**. It may be that the reaction proceeds *via* the hydrogen-bonded (HB) intermediate **6**.[8]

The possibility of the second path, a similar path for ester hydrolysis in the gas phase, was proposed by Takashima[9] and proved by Hori[8] with the help of *ab initio* MO calculations.

† 1 kcal mol$^{-1}$ = 4.184 kJ mol$^{-1}$.

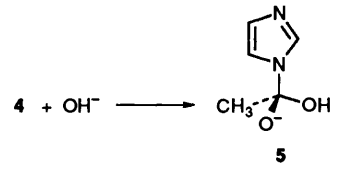


(3)

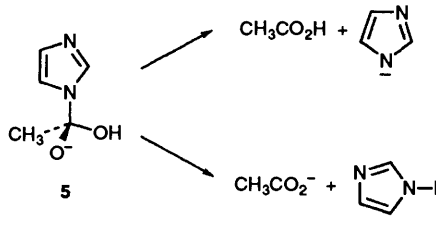


(4-1)

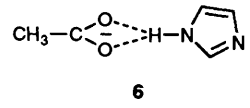


(4-2)

*N*-Acylimidazole in the surfactants with alkoxy fragments was also observed to deacylate increasingly rapidly,[10] the reasons for which still remain to be identified, intriguing as it may be. Therefore, the reaction for methyl acetate **1a** was also computed in order to simulate the way *N*-acylimidazole in the surfactants reacts with alcohol fragments.

Hydrolysis in micelles is not affected very much by solvents since the reaction proceeds in hydrophobic environments. Moreover, this phenomenon is governed by the enthalpy of the reaction, not by the entropy.[11] Theoretical calculations, therefore, are useful for investigating hydrolysis in micelles: molecular mechanics (MM)[12] and molecular dynamic (MD)[13] calculations were used to investigate the enantio-recognition of functional catalysis. MO calculations are also a very powerful tool to deal with such systems. In the present study, by using *ab initio* MO calculations we delved into the hydrolysis mechanism of AcONp and *N*-acetylimidazole as a model reaction for those taking place in the micelles, and for those processes in the micellar catalytic system given by eqns. (1)–(4). The relative permittivity $\varepsilon$ in micelles is estimated to be around 30–40.[14] Moss *et al.* identified the micelle systems with the different relative permittivities of 3 and 30 along with a distant dependent dielectric.[12a] The change in the values did not bring about a remarkable difference in the energy ordering of the various conformers whereas a change in the energies took place between any two conformations. Bearing in mind the kind of effect that might be caused by the surfactants on the reaction, we expected our investigations to provide us with an insight into what is going on in the micellar system.

*Method of Calculation.*—The *ab initio* MO calculations were carried out with the GAUSSIAN86 program[15] at the Institute for Molecular Science and the GAUSSIAN90 program[16] for Fujitsu S4/2 (SUN SPARCstation) computers. Molecular geometries including transition states (TS) were optimized by the energy gradient method and checked with vibration frequency calculations. The intrinsic reaction coordinate[17] (IRC) was calculated in order to check and obtain a profile of the proposed reaction. The 6-31G basis set,[18] a small one, served for the geometry optimization because the model molecules are too big to perform *ab initio* MO calculations with larger ones. The MP2/6-31 + G//RHF/6-31G energies (the larger basis set) were also estimated so that a better description might be had of energies concerned with the molecules under consideration.

The total energies, according to the RHF/6-31G (MP2/6-31 + G//RHF/6-31G) calculations, were −75.31175 (−75.51630), −266.70735 (−267.23992) and −342.09571 (−342.79398) Hartree for $OH^-$, **1a** and **8**, respectively.* The stabilization, when the TD intermediate **8** was formed, turned out to be 48.1 (23.7) kcal $mol^{-1}$. The small basis set produced a calculation value of 24.4 kcal $mol^{-1}$, an overestimation *vis-à-vis* the larger set. As shown in Fig. 7, a similar overestimation of 21.3 kcal $mol^{-1}$ is reported for the *N*-acetylimidazole and OH case. This difference came from the so-called basis set superposition error.[19] As regards the other energies, however, the small basis set calculations did not differ from the larger. Thus the better calculated energies are used in discussing the small systems.

## Results and Discussion

*Reaction of Methyl or* p-*Nitrophenyl Acetate Catalysed by Imidazolyl Anion.*—It is of importance to note that neither AcONp nor methyl acetate could form TD intermediates with imidazole according to the present MO calculations. This agrees with the experimental results obtained by Takagi and his coworkers,[7c] who failed to observe the formation of acylimidazole derivatives when they used *N*-octylimidazole, **7**,

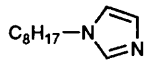


**7**

as the catalyst in the surfactant system. This molecule is incapable of forming an anion, unlike imidazole, and the basicity of the neutral form is too weak to form TD intermediates, which, in contrast, were optimized through the calculations of the imidazolyl anion and the esters. Both we[5,6] and others[7] have observed the acylimidazole intermediates when imidazolyl derivatives were used as the catalysts, because the intermediates have imidazolyl fragments that are able to form the anion.

The first process is, to a great extent, dependent on the pH used for the reaction.[5] In solution with a pH higher than 8, the imidazole fragment in the catalyst ought to be negatively charged before it participates in forming the cosurfactants. In the lower pH region, the environmental effect lowers the $pK_a$ of acids[14] and a similar effect is expected to be obtained in the case of imidazoles in the micelle system under consideration. The imidazole fragment of the histidine residue seems to have a negative charge when forming TD intermediates. For this reason we used the imidazoyl anion as the nucleophile to attack the esters.

Fig. 1 displays the optimized geometries of the molecules related to the first process. Lengths C(2)–O(4) in **1a** and **1b** were calculated, producing the values of 1.348 and 1.365 Å, respectively, and the discrepancy spans 0.017 Å. The bond as it is in **1b** is weak even in the ester form. This weakness is intensified in TD intermediates. Bond length C(2)–O(4) in **3a** was calculated to be 1.472 Å, almost the same as the TD intermediate **8** with methyl acetate and OH (1.437 Å). Complex **3a**, proving to be 1.308 Å for C(2)–O(1), differs from **8** (1.313 Å) only by 0.005 Å. Although methyl acetate forms TD intermediates with different nucleophiles such as OH and the imidazoyl anion, **3a** is almost the same as **8** in its basic

* The calculated total energies in Hartree are as follows; **1b**: −660.50659, **2**: −224.11344 (−224.63876), **3a**: −490.83374 (−491.89643), **3b**: −884.67046 and **4**: −376.41302 (−377.21444). Values in parentheses are the energies estimated by MP2/6-31 + G//RHF/6-31G calculations. We could not obtain the MP2/6-31 + G//RHF/6-31G energies for **1b** and **3b**.

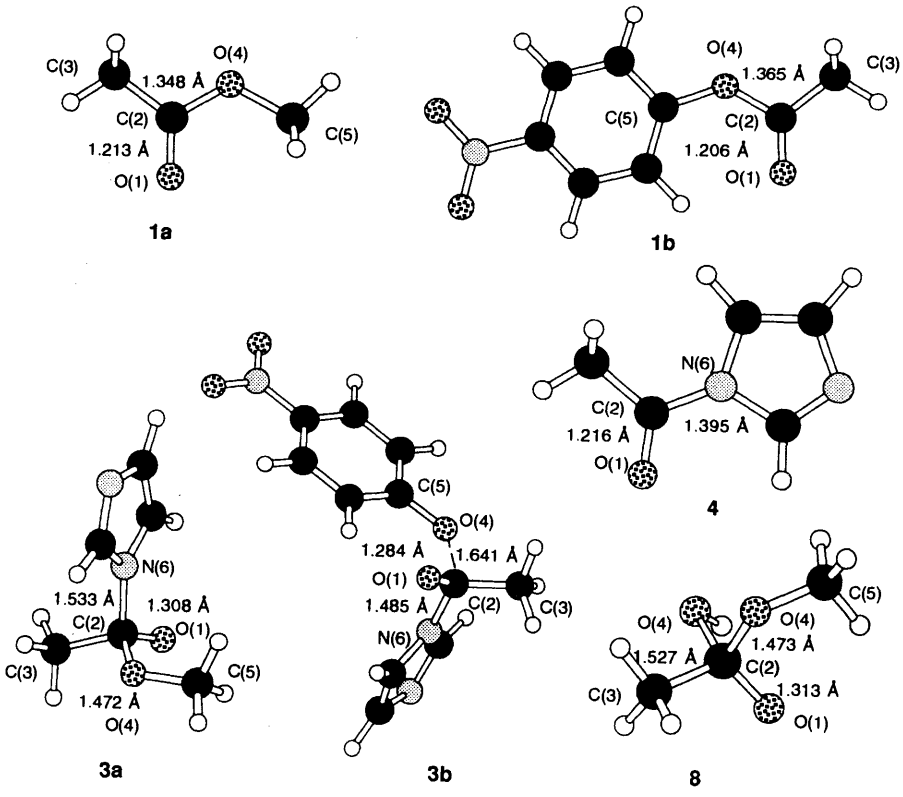


**Fig. 1** Optimized geometries of the related molecules for the first process using *ab initio* calculations with the 6-31G basis set

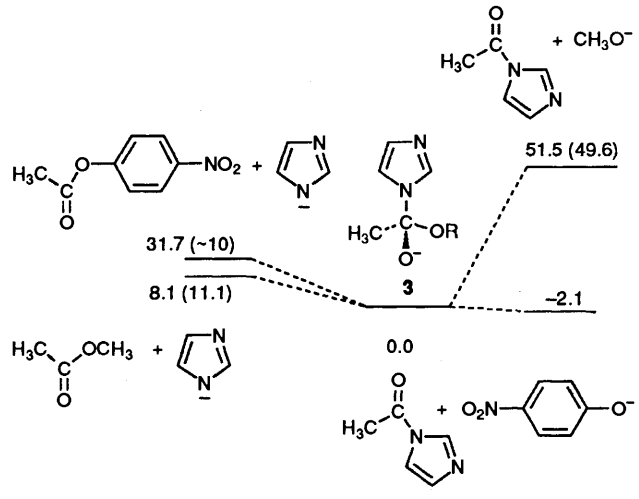


**Fig. 2** Energy correlation diagram (kcal mol$^{-1}$) for the first process calculated by the 6-31G (MP2/6-31 + G//RHF/6-31 + G) calculations. The values in the diagram are relative to the energy of **3a** or **3b**.

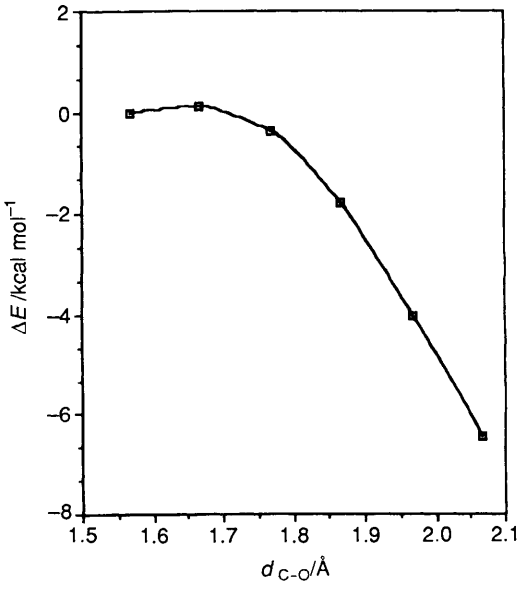


**Fig. 3** Potential energy profile of the decomposition of **3b** along the C(2)–O(4) bond breaking estimated by AM1 calculations

structures. That they have disparate alkoxide fragments causes **3a** and **3b** to differ hugely from each other: $CH_3O$ and *p*-$NO_2C_6H_4O$ being the alkoxide fragments in question. Along with this, intermediate **3b** has a C(2)–O(4) bond (1.641 Å) longer by 0.169 Å than does **3a**, whereas it has a C(2)–N(6) bond (1.485 Å) shorter by 0.048 Å *vis-à-vis* **3a** (1.533 Å). Bond length C(2)–O(1) in **3b**, being 1.284 Å, has slight double-bond nature.

The formation of **3a** releases an amount of stabilization energy as small as 11.1 kcal mol$^{-1}$ as illustrated in Fig. 2. By estimation formation of **3b** turned out to be exothermic by 31.7 kcal mol$^{-1}$ with the 6-31G basis set. As discussed above, this small basis set calculation, however, resulted in an excess of *ca.* 20 kcal mol$^{-1}$ in estimating the stabilization energy when they were compared with the MP2/6-31 + G//RHF/6-31G level calculations. It follows that the estimated energy for AcONp is *ca.* 10 kcal mol$^{-1}$, which is similar to that for the TD intermediate **3a** proceeding from methyl acetate and the imidazolyl anion. The decomposition of **3b** is exothermic, but only to a slight extent (*i.e.* 2.1 kcal mol$^{-1}$, RHF/6-31G calculation). This characteristic is unique to AcONp in that usually esters decompose into a carboxylic acid and an alkoxide ion in a way which is endothermic by more than 30 kcal mol$^{-1}$.[20]

Calculation with the AM1 Hamiltonian[21] was made on the potential surface along the increasing C–O bond length for the reason that **3b** is too large for all of its geometries to be optimised (with *ab initio* MO calculations). As shown in Fig. 3,

**Table 1** Geometrical parameters[a] for the TD and HB intermediates together with those along the IRC of the decomposition for the second step

| | TD | $s$ = 0.0 (TS) | $s$ = 8.87 | HB |
|---|---|---|---|---|
| O(1)–C(2) | 1.313 | 1.246 | 1.210 | 1.253 |
| C(2)–O(4) | 1.464 | 1.394 | 1.367 | 1.275 |
| O(4)–H(5) | 0.953 | 0.952 | 0.977 | 1.709 |
| C(2)–N(6) | 1.527 | 2.000 | 2.814 | 3.388 |
| H(5)–N(6) | 2.803 | 2.799 | 1.956 | 1.026 |
| O(1)–C(2)–O(4) | 113.2 | 118.9 | 122.0 | 126.2 |
| ∠C(2)–O(4)–H(5) | 105.7 | 109.8 | 113.6 | 112.2 |
| ∠O(1)–C(2)–C(3)–O(4) | −125.6 | −146.7 | −179.1 | −179.6 |

[a] Values for lengths and angles are given in Å and deg.

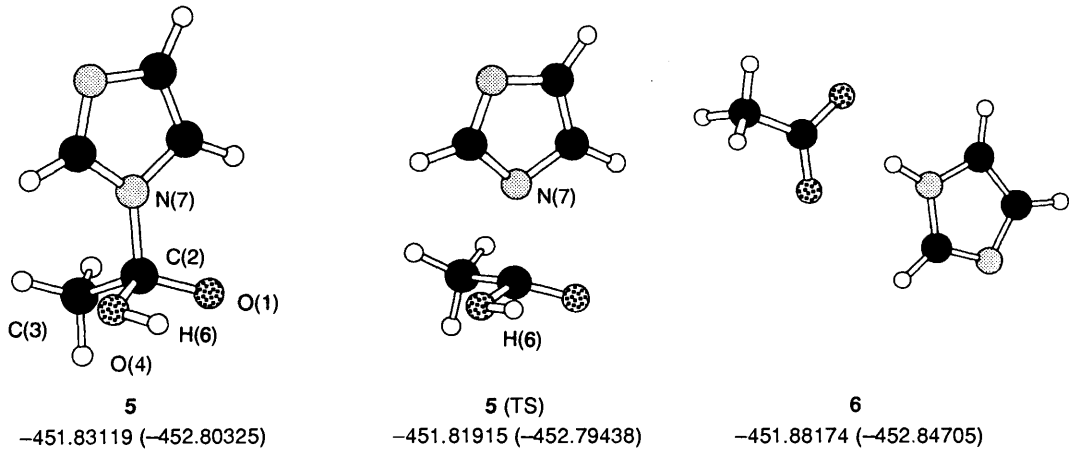


**Fig. 4** Optimized structures of the TD intermediate **5**, the transition state **5** (TS) and the HB intermediate **6** of the second process. Values under the numbers for the geometry are the total energies estimated by RHF/6-31G (MP2/6-31 + G//RHF/6-31G) calculations.

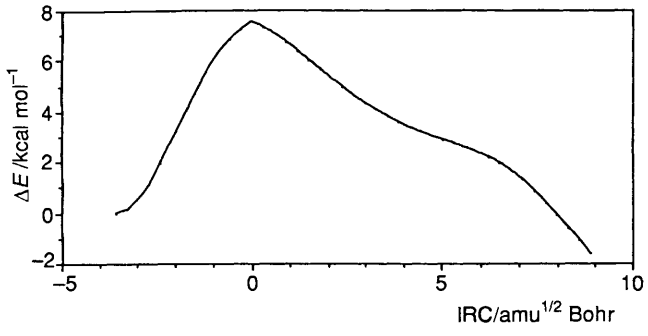


**Fig. 5** The potential energy profile of the decomposition of the TD intermediate along the IRC for eqn. (4-2)

the potential curve has no significant barrier along the elongation of the bond. The calculation suggests that the decomposition of **3b** occurs instantly after the TD intermediate is formed. This energetic feature relates very much to the nature of $p$-$NO_2C_6H_4O$, a good leaving group.

In the previous investigation, it was mentioned that greater affinity to the micelle system used at that time was attributed to the D-form substrates than to the L-form molecules whereas the L-form substrates decomposed faster than the D-form substrates.[22] The previous experiments estimated the activation energies of the first process and obtained values of 7 ~ 10 kcal $mol^{-1}$. The present MO calculations, however, show that the TD intermediates **5** form with no remarkable barrier in the gas phase. This disparity probably arises from the geometric features of the dipeptide catalysis and of the substrates. Such theoretical and experimental results corroborate the concept that the enantioselectivity of the catalytic system originates in the process in which the formation of TD intermediates takes place.

*Hydrolysis of* N-*Acetylimidazole by Hydroxide Ions*.—The model reactions of the second process are represented in eqns. (3) and (4). Two possibilities exist for eqn. (4). One is the normal ester hydrolysis as given in eqn. (4-1). The other is that given in eqn. (4-2) and proposed by Takashima *et al.*[9] and Hori,[8] involving the decomposition of the TD intermediate. Application of the latter mechanism to the hydrolysis in the model systems was of great interest.

In Fig. 4 the geometries are drawn of the TD and HB intermediates along with the TS for path (4-2). Structure **5** (TS), whose imaginary frequency is 249.1i $cm^{-1}$, determines the geometry to be in a transitional state. It is not expected that the H(6) of the HO fragment in **5** (TS) transfers to N(7) of the imidazolyl fragment during the reaction because the N(7)–H(6) is as far apart as 2.799 Å as listed in Table 1. For this reason we made use of this TS geometry to calculate the IRC, along which the potential energy profile is shown in Fig. 5. The energy value around $s$ = −3.5 is almost the same as that of **5**. The energy increases sharply before the TS and thereafter declines to a gentle curve. Note that somewhere around $s$ = 8.0 the energy is nearly the same as in the TD intermediate **5**. Further IRC calculations may show a decrease which may correspond to a difference between **5** and **6**.

The dihedral angle ∠O(1)–C(2)–C(3)–O(4) indicates to what extent hybridization ($sp^2$: 180.0°, $sp^3$: 109.5°) of the C(2) occurs. The angle in the TS geometry being −146.7°, Table 1, C(2) largely retains its $sp^3$ nature, whereas it has perfect $sp^2$ hybridization at $s$ = 8.87, the calculated angle being −179.1°. That the length is 2.799 Å prevents H(6) from interacting with N(7) in the TS. The length at $s$ = 8.87 Å is 1.956 Å and the lighter atom is able to move over to N(7), forming a new N–H bond. Fig. 6 illustrates this change in the geometry along the IRC.

As far as the present hydrolysis is concerned, the potential energy was as expected, as was the case in our previous study.[8]

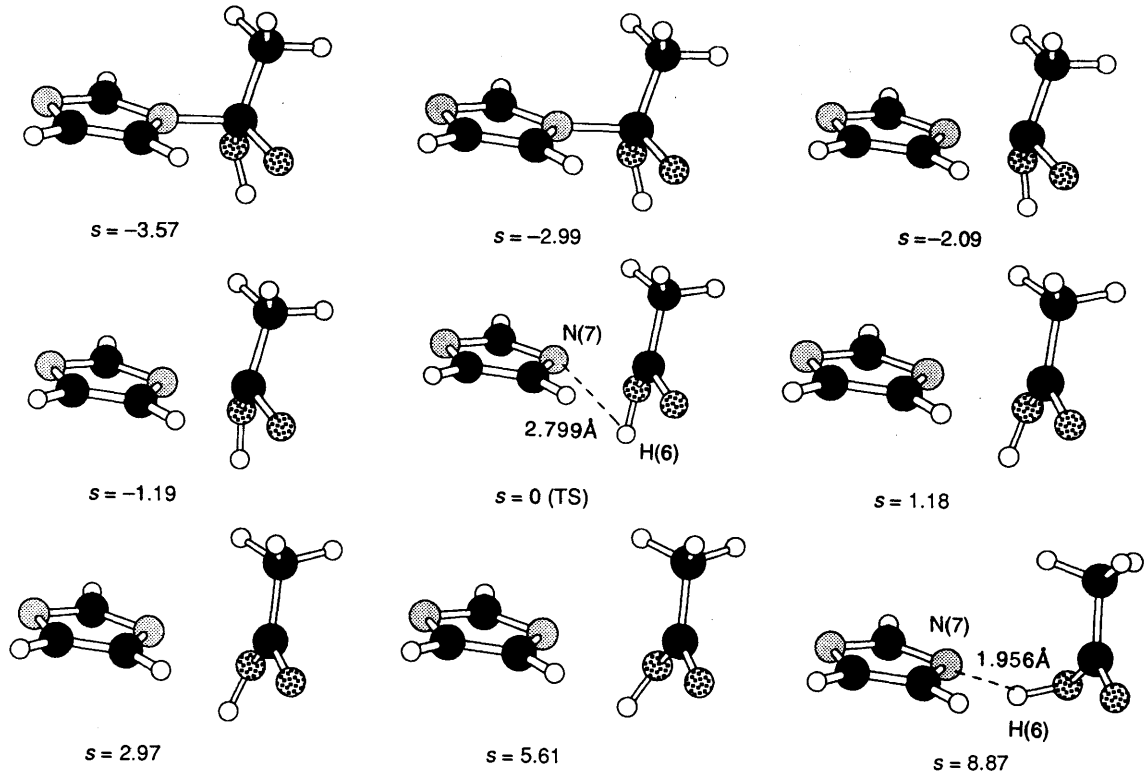


**Fig. 6** The change of geometry for the decomposition of the TD intermediate **5** along the IRC for eqn. (4-2)

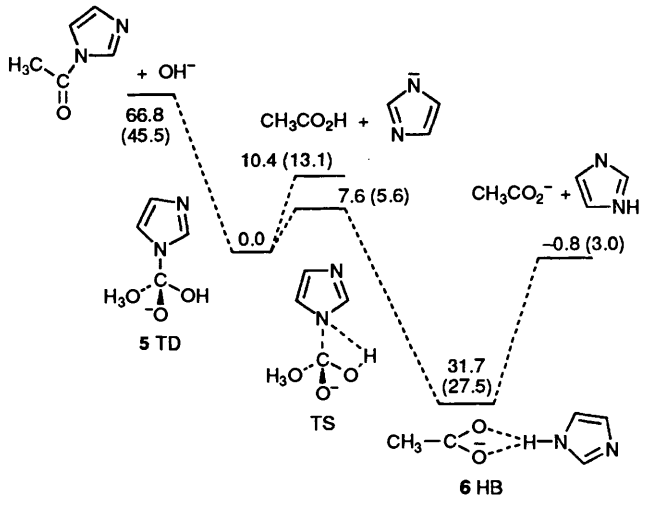


**Fig. 7** Energy correlation diagram of the second process estimated by the RHF/6-31G (MP2/6-31 + G//RHF/6-31G) calculations. The values in the diagram are relative to the energy of **5**.

A change in energy accompanies the transfer of the hydrogen atom in the HO fragment to the alkoxide fragment. Therefore, a similar change in geometry might be expected here as the present system goes beyond $s = 8.0$.

Fig. 7 shows the energy correlation diagram for the two proposed paths. The formation of the TD intermediate is exothermic by 45.5 kcal mol$^{-1}$ (MP2/6-31 + G//RHF/6-31G calculation); the acetic acid–imidazolyl anion system, both being products, is higher in energy than the TD intermediate by 13.1 kcal mol$^{-1}$. The hydrophobic micelles are considered to resemble the gas phase in terms of the energy relation, the C–N bond breaking of **8** has an activation energy that is either equal to or a little over the difference value of the energy. On the other hand, the carboxylate ion–imidazole system has almost the same stability as the TD intermediate, the difference in energy being as little as 3.0 kcal mol$^{-1}$. The HB intermediate shown in Fig. 7 is more stable than the TD intermediate by 27.5 kcal mol$^{-1}$, and its activation energy was calculated to be 5.6 kcal mol$^{-1}$, which is less than half the energy difference (13.1 kcal mol$^{-1}$) between the TD intermediate and the combination of acetic acid and the imidazolyl anion.

Madula and Jorgensen,[23] who resorted to *ab initio* and Monte Carlo calculations, studied the OH + $H_2CO$ system and estimated the free energy barrier, obtaining the same value of 25 kcal mol$^{-1}$ that is needed to form the TD intermediate. The barrier, caused mainly by desolvation of the OH anion, was an overestimation, an excess of 5–10 kcal mol$^{-1}$. However, it takes more energy to desolvate the OH anion and extract it into micelles than to activate the two paths. Thus, both the paths were considered to be highly feasible for the decomposition mechanism of the TD intermediate **5** in micelles.

*The Acceleration of the Deacylation Process due to the Alkoxide Fragment in the Surfactant.*—It is usual that the micellar system does not work well as a catalyst for the deacylation of *N*-acylimidazole (the second process). The reaction is made 20–50 times quicker by the presence of surfactants with alcohol fragments than by those with other functional groups. Fig. 2 also illustrates the functionalized micelles, where the methoxide ion is the model of the alkoxide ion attached to N atoms on the surfactants. The TD intermediate **3a** forms where *N*-acetylimidazole and the methoxide ion react together. The newly formed intermediate is more stable than the reactants by 49.6 (MP2/6-31 + G//RHF/6-31G) kcal mol$^{-1}$. Decomposition of the TD intermediate triggers formation of imidazolyl anion and methyl acetate, the products of which formation are slightly less stable than **3a** by 11.1 kcal mol$^{-1}$. On the other hand, the energy correlation is similar to the alkoxide case in which the TD intermediate **5** forms exothermically by 66.8 kcal mol$^{-1}$ with *N*-acetylimidazole and OH, and decomposes endothermically

by 10.4 kcal $mol^{-1}$ to acetic acid and the imidazolyl anion (Fig. 7). However, the process of TD intermediate formation needs an activation barrier, requiring $OH^-$ to be extracted from the liquid phase, unlike the system with alkoxide fragments on the surfactants. Therefore, the second deacylation is accelerated by the presence of the alcohol moiety in the surfactants.

*Concluding Remarks.*—The present study has been an attempt to elucidate the mechanism of ester hydrolysis in micellar catalysis, using model systems constructed by *ab initio* MO calculations. (*i*) The basicity of neutral imidazole, because it is very weak, prevents the formation of a TD intermediate. Thus, the imidazolyl fragment in the dipeptide catalysis, when it plays the role of the active species for ester hydrolysis, needs to be either negatively charged or, at least, activated by the carboxylate fragment in the peptide. (*ii*) TD intermediate formation in the first process governs the observed enantioselectivity of micellar catalysis. (*iii*) In the second process, *N*-acetylimidazole reacts with the OH ion coming from the liquid phase. Two paths were examined to see how they might be involved in the decomposition of the TD intermediate. Both processes require an activation energy which is considered to be smaller than the energy to desolvate the OH ion, though the mechanism represented by eqn. (4-2) has a lower activation energy by 7.5 kcal $mol^{-1}$ than the path in eqn. (4-1) according to MP2/6-31 + G//RHF/6-31G level calculations.

## Acknowledgements

The authors thank the Computer Center, Institute for Molecular Science at the Okazaki National Research Institutes for the use of the HITAC M-680 and S-820/80 computers and the Library Program GAUSSIAN86. This work is supported by a Grant-in-Aid for Scientific Research from the Ministry of Education of Japan.

## References

1 J. H. Fendler and E. J. Fendler, *Catalysis in Micellar and Macromolecular Systems*, Academic Press, New York, 1975; R. A. Moss, R. C. Nahas and S. Rawaswami, *J. Am. Chem. Soc.*, 1977, **99**, 672; U. Tonellato, *J. Chem. Soc., Perkin Trans. 2*, 1977, 821; C. Gitler and A. Ocha-Solano, *J. Am. Chem. Soc.*, 1968, **90**, 5004; W. Takagi, S. Kobayashi and D. Fukushima, *J. Chem. Soc., Chem. Commun.*, 1977, 29.

2 Y. Ihara, *J. Chem. Soc., Chem. Commun.*, 1978, 984; Y. Ihara, *J. Chem. Soc., Perkin Trans. 2*, 1980, 1483; Y. Ihara, M. Nango and N. Kuroki, *J. Org. Chem.*, 1980, **54**, 5011; Y. Ihara and R. Hosako, *Bull. Chem. Soc. Jpn.*, 1982, **55**, 1979; Y. Ihara, R. Hosako, M. Nango and N. Kuroki, *J. Chem. Soc., Perkin Trans. 2*, 1983, 5.

3 K. Ohkubo, H. Ishida, K. Yamaki and M. Kawata, *Chem. Lett.*, 1991, 1723; K. Ohkubo, M. Kawata, T. Orito and H. Ishida, *J. Chem. Soc., Perkin Trans. 1*, 1989, 666; K. Ohkubo and S. Miyake, *J. Chem. Soc., Perkin Trans. 2*, 1987, 995; K. Ohkubo, K. Hirayama and K. Yamaki, *Isr. J. Chem.*, 1985, **25**, 282.

4 R. Ueoka, Y. Matsumoto, T. Yoshino, T. Hirose, J. Kikuchi and Y. Murakami, *Chem. Lett.*, 1986, 127; R. Ueoka, Y. Matsumoto, T. Yoshino, N. Watanabe, K. Omura and Y. Murakami, *Chem. Lett.*, 1986, 1743; R. Ueoka, Y. Matsumoto, R. A. Moss, S. Swarup, A. Sugii, K. Harada, J. Kikuchi and Y. Murakami, *J. Am. Chem. Soc.*, 1988, **110**, 1588.

5 Y. Ihara, R. Hosako, M. Nango and N. Kuroki, *J. Chem. Soc., Perkin Trans. 2*, 1983, 5.

6 (*a*) Y. Ihara, Y. Kimura, M. Nango and N. Kuroki, *Macromol. Chem.*, 1982, **3**, 521; (*b*) Y. Ihara, Y. Kimura, M. Nango and N. Kuroki, *Bioorg. Chem.*, 1985, **13**, 88.

7 (*a*) R. A. Moss, R. C. Nahas and S. Ramaswami, *J. Am. Chem. Soc.*, 1977, **99**, 67; (*b*) U. Tonellato, *J. Chem. Soc., Perkin Trans. 2*, 1977, 821; (*c*) W. Takagi, S. Kobayashi and D. Fukushima, *J. Chem. Soc., Chem. Commun.*, 1977, 29; (*d*) W. Takagi, D. Fukushima, T. Eiki and Y. Yano, *J. Org. Chem.*, 1979, **44**, 555.

8 K. Hori, *J. Chem. Soc., Perkin Trans. 2*, 1992, 1629.

9 K. Takashima, S. M. Jose, A. T. do Amaral and J. M. Riveros, *J. Chem. Soc., Chem. Commun.*, 1983, 1255.

10 Y. Ihara, M. Nango, Y. Kimura and N. Kuroki, *J. Am. Chem. Soc.*, 1983, **105**, 1252.

11 R. Ueoka and Y. Matsumoto, *J. Synth. Org. Chem. Jpn.*, 1987, **25**, 312.

12 (*a*) R. A. Moss, T. F. Hendrickson, R. Ueoka, K. Y. Kim and P. K. Weiner, *J. Am. Chem. Soc.*, 1987, **109**, 4363; (*b*) Y. Ihara, S. Asakawa, K. Igata, Y. Matsumoto and R. Ueoka, *J. Chem. Soc., Perkin Trans. 2*, 1991, 543.

13 K. Ohkubo, *Kagaku*, 1992, **47**, 466.

14 J. H. Fendler, *Membrane Mimetic Chemistry*, Wiley, New York, 1982, p. 19.

15 GAUSSIAN 86: M. J. Frisch, J. S. Binkley, H. B. Schlegel, K. Raghavachari, C. F. Melius, R. L. Martin, J. J. P. Stewart, F. W. Bobrowicz, C. M. Rohlfing, R. L. Kahn, D. J. Defrees, R. Seger, R. A. Whiteside, D. J. Fox, E. M. Fluder, S. Topiol and J. A. Pople, Carnegie-Mellon Quantum Chemistry Publishing Unit, Carnegie-Mellon University, Pittsburgh PA 15213; N. Koga, S. Yabushita, K. Sawabe and K. Morokuma, GAUSSIAN86, Institute for Molecular Science.

16 GAUSSIAN 90, Revision G, M. J. Frisch, M. Head-Gordon, G. W. Trucks, J. B. Foresman, H. B. Schlegel, K. Raghavachari, M. Robb, J. S. Binkley, C. Gonzalez, C. Defrees, D. J. Fox, R. A. Whiteside, R. Seeger, C. F. Melius, J. Baker, R. L. Martin, L. R. Kahn, J. J. P. Stewart, S. Topiol and J. A. Pople, Gaussian, Inc., Pittsburgh PA, 1990.

17 K. Fukui, *Acc. Chem. Res.*, 1981, **14**, 363; M. Head-Gordon and J. A. Pople, *J. Chem. Phys.*, 1988, **89**, 5777.

18 W. J. Hehre, R. Ditchfield and J. A. Pople, *J. Chem. Phys.*, 1972, **56**, 2257.

19 F. Boys and F. Bernardi, *Mol. Phys.*, 1970, **19**, 553; G. Karlstrom and A. J. Sadlej, *Theor. Chim. Acta*, 1982, **61**, 1.

20 C. S. Ewig and J. R. Van Wazer, *J. Am. Chem. Soc.*, 1986, **108**, 4774; M. J. S. Dewar and D. M. Storch, *J. Chem. Soc., Chem. Commun.*, 1985, 94; M. J. S. Dewar and D. M. Storch, *J. Chem. Soc., Perkin Trans. 2*, 1989, 877.

21 M. J. S. Dewar, E. G. Zoebisch, E. F. Healy and J. J. P. Stewart, *J. Am. Chem. Soc.*, 1985, **107**, 3902.

22 R. Ueoka, Y. Matsumoto, Y. Ninomiya, K. Inoue and K. Ohkubo, *Chem. Lett.*, 1981, 785; R. Ueoka and Y. Murakami, *J. Chem. Soc., Perkin Trans. 2*, 1983, 219; Y. Ihara, N. Kunikiyo and M. Nango, *J. Chem. Soc., Perkin Trans. 2*, 1983, 1741.

23 J. D. Madura and W. L. Jorgensen, *J. Am. Chem. Soc.*, 1986, **108**, 2517.

*Paper* 3/07635K
*Received* 30*th December* 1993
*Accepted* 9*th May* 1994